

Biologically Inspired Adhesion based Surface Climbing Robots

Carlo Menon

CISAS "G. Colombo"
University of Padova, 35131 Padova, Italy
menoncarlo@stargatenet.it

Metin Sitti

Department of Mechanical Engineering
Carnegie Mellon University, Pittsburgh, PA 15213, USA
sitti@cmu.edu

Abstract— Climbing robots can perform many tasks inaccessible to other robots or humans such as inspection, repair, cleaning, surveillance, and exploration. This paper presents and discusses the design, fabrication, and evaluation of two novel bio-inspired climbing robots. Both are inspired by the locomotion of Geckos, a highly skilled natural climber. They are developed for terrestrial and extra-terrestrial environments, and their kinematics is inspired by the Geckos' gait. The first relatively large robot actuated by conventional motors is designed to operate at both in Earth and space scenarios. The second robot, whose motion is controlled using shape memory alloy actuators and size can be miniaturized to few centimeters scale, is designed for terrestrial applications. Preliminary prototypes of these robots are developed, demonstrated, and evaluated by steep and flat acrylic surface climbing tests. Current robots can successfully climb up to 65° slopes at 2 cm/sec speeds.

Index Terms— Biomimetic robots, climbing robots, micro/nanorobots, space robots

I INTRODUCTION

The locomotion, sensing, navigation, and adaptation capabilities in animals have long inspired researchers in robotic system design. The purpose of this study is to determine the potential of climbing robots for both terrestrial and extra-terrestrial applications. The development of climbing robots is mainly driven by automating tasks which are currently accomplished manually at a risk to the human workers. Robots could reduce the risk to humans in many different applications. Moreover, the ability to climb surfaces and walk are also crucial for inspection and maintenance of space shuttles, satellites, nuclear plants [1], search-and-rescue for homeland security [2], cleaning and painting [3], exploration on planets or hazardous regions, and micro/nano-scale manufacturing applications [4]. These autonomous robots encounter mostly unstructured environments, only accessible by legged locomotion and, in particular, climbing. Many legged animals, e.g., cockroaches, beetles, ants, and crickets [5], have walking abilities which have been studied to develop a new generation of mobile robots. Geckos' climbing ability has attracted scientists' attention since they can adhere to most surfaces robustly and climb with very high maneuverability and agility [6].

This paper proposes Gecko inspired climbing robots for applications in unstructured environments. Design, fabrication and test phases of two robot prototypes are

presented. The first robot, called the Rigid Gecko Robot (RGR), has been designed for operating in space environments. Reliability and robustness are the most important requirements for the RGR. The second robot, called the Compliant Gecko Robot (CGR), has been designed using unconventional technologies which will allow robot miniaturization. The CGR prototype has a composite structure and its Gecko mimicking locomotion relies on shape memory alloy wire actuators.

II ROBOT DESIGN

Geckos differ from other climbing animals especially for their adhesion system and locomotion. In this section, the strategy for developing a Gecko inspired attachment pad, feet, and robot prototype is presented and discussed.

II.A Adhesive Pad and Foot Design

Much work has been devoted to the development of attachment mechanisms for climbing robots. Suction based attachment [7] requires the robot to carry an onboard pump to create a vacuum inside cups which are pressed against the wall or ceiling. However, this mechanism is slow, consumes high power, does not work in space environment, and any gap in the seal can cause the robot to fall. Another attachment mechanism relies on magnetic adhesion [8]. Magnetic attachment is possible only in very specific environments, e.g., nuclear facilities, where the surface is ferromagnetic. Thus, this solution is unsuitable for many applications.

Another strategy is to study *passive* attachment mechanisms, like those used by climbing animals. The *Tokay* Gecko, for example, can weigh up to 300 grams and reach lengths of 35cm, yet is still able to run inverted and cling to smooth and rough walls. Unique adhesive pads allow Geckos' incredible climbing performance without contaminating the surrounding environment. Synthetic dry fibrillar adhesive has been developed to mimic the Gecko adhesive pad structure with promising initial results. Using micro-molding techniques, 4μm diameter micro-fibers have been obtained [9]. This fibrillar adhesive, however, is still under development and does not yet achieve as high performances as other soft and dry adhesives. Synthetic gecko adhesive was tested and compared to soft adhesives such as Silly Putty® and flat polydimethyl siloxane (PDMS). Fig. 1 shows results obtained using a customized tensile adhesion measurement test-bed. Adhesives had a

size of 95mm^2 . They were loaded against a glass surface with a preload of 75mN , an approach velocity of 0.08mm/s , and a retracting velocity of 0.4mm/s . The contact time was 1s .

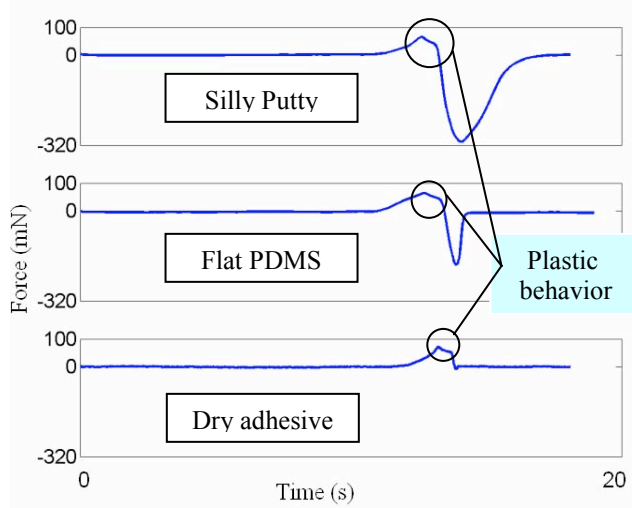


Fig. 1 Adhesion behavior of various soft and fibrillar adhesives under 75mN preload and 1s contact time.

Fig. 1 also shows that Silly Putty® exerts the highest normal adhesive force and it was therefore chosen for our robotic application.

II.B Rigid Gecko Robot Design

In this section, the kinematics and dynamics of the Rigid Gecko Robot are discussed. Fig. 2 shows the two-dimensional kinematic model of the RGR prototype. The robot has ten degrees of freedom (DOF), as shown in the left side of Fig. 2. The first four-DOFs (numbers 1, 2, 3, 4 in Fig. 2) are used for lifting robotic legs by means of four motors; one-DOF (number 5), in the middle of the robot's back, is necessary for robot locomotion and it is controlled using another motor. The other five-DOFs are passive revolute joints. The right side of Fig. 2 shows that the planar kinematics of the robot can be represented by a four-bar-linkage.

The dynamics of the RGR in vertical climbing mode were studied using multi-body software (VisualNastran Desktop 4D), and a three-dimensional robot model with realistic specifications. The robot model was 10cm long, 10cm wide, and it weighed 80g . The rotation of the motor controlling the robot's back displacements (number 5 in Fig. 2) was the input for the dynamic simulation.

Fig. 3 shows the torque output for the same motor. This torque was necessary for counterbalancing the weight and dynamic forces caused by the robot motion.

Fig. 4 shows both the robot model and the adhesive forces required by the most stressed robot foot. The shear forces, F_y and F_z , are bigger than the normal force, F_x . The total force is 1.5N .

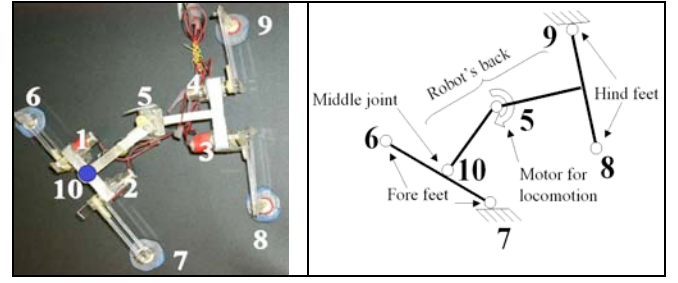


Fig. 2 Pictures of Gecko Robot prototypes.

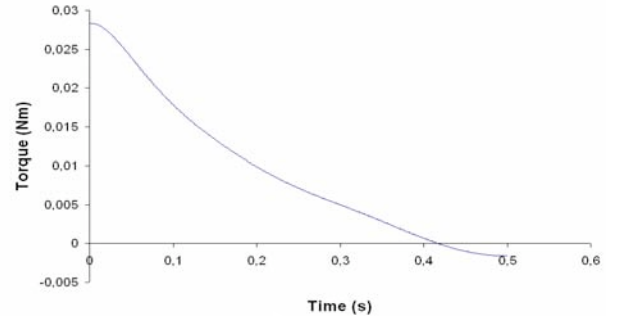


Fig. 3 Output for the multi-body software: torque for the motor positioned on the middle of the gecko robot back

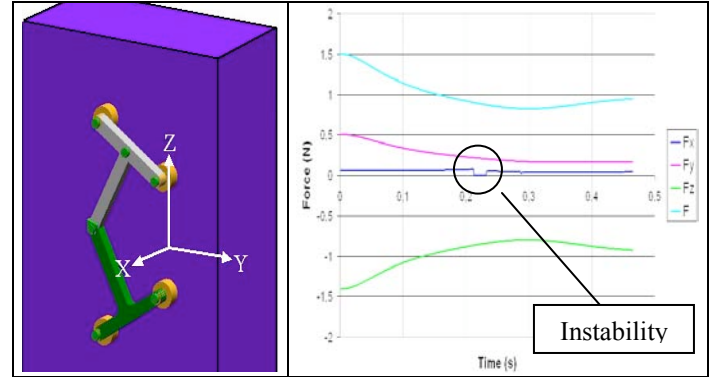


Fig. 4 Rigid Gecko Robot simulated dynamic analysis: left: RGR model; right: robot foot forces during vertical climbing phase

The results of the multi-body software analysis were used to select the adhesive pad size. Since the adhesive material, Silly Putty®, has a plastic behavior, the Bowden Tabor equation holds:

$$F_t = \tau \cdot A_c \quad (1)$$

The necessary contact area was determined to be 6cm^2 .

Dynamic simulation results show numerical instabilities after 0.22s and 0.25s (right side of Fig. 4). The robot position which causes these instabilities is shown in the left side of Fig. 5. If the Back Revolute Joint (BRJ) is controlled by motor torque, three *passive* revolute joints are affected by dynamic loads: the Middle Revolute Joint (MRJ), the Hind Revolute Joint (HRJ) and the Fore Revolute Joint (FRJ), which represents the feet in contact with the vertical surface. The robotic model can thus be simplified in a three-bar-linkage as shown in the right side of Fig. 5. For small displacements, this configuration has an additional redundant DOF which makes the robot motion unstable [10]. In the real robot prototype,

mechanical joint clearances amplify instability effects thus compromising the robot climbing performance.

Robot kinematic analysis shows that the instable configuration is avoided by:

1. Increasing the length of fore legs.
2. Decreasing the length of hind legs.
3. Changing the position of the motor.
4. Decreasing the angle range of the BRJ rotation.

For the RGR prototype, the fourth solution was chosen since a symmetrical configuration of the robot was preferred.

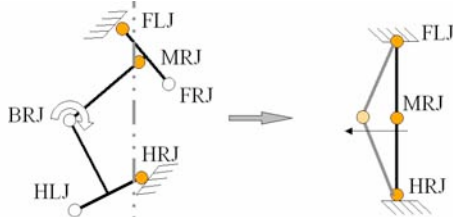


Fig. 5 On the left, the RGR is represented in its unstable configuration; on the right, a schematic representation of the gecko robot showing the model to be studied for understanding its unstable configuration. (FLJ=Fore Left Joint; HRJ=Hind Right Joint; FRJ=Fore Right Joint; HLJ=Hind Right Joint; BRJ=Back Right Joint)

II.C Compliant Gecko Robot Design

A new compliant system has been developed for the CGR in order to facilitate future design of miniaturized climbing robots. This robot has a composite material frame and shape memory alloy (SMA) wires provide motion that mimics gecko muscles. The compliant robotic back (Fig. 6) is flexible, and SMA wires are attached to both sides. The flexible robot back is able to recover the initial length of the SMA wires during their cooling phase. This system is used to locomote the CGR.

The geometry of the robot was optimized both to have long robot steps and amplify SMA wires' force. With regard to robot step optimization, analytical kinematic equations were derived taking into account flexible robotic back characteristics.

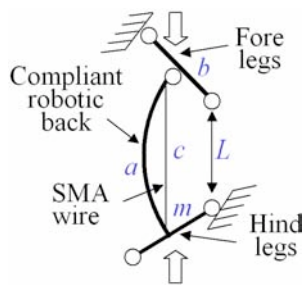


Fig. 6 Compliant Gecko Robot model

Analysis was necessary to obtain ΔL , the robot step length, as a function of all the other parameters, a , b , c , and m of Fig. 6. In order to compare the effects of a and m and obtain the corresponding physical solution, the condition $a+m=\text{constant}$ was used. In addition, the maximum contraction of the wires was limited to the 4% of their length because of the inherent SMA wire characteristics. For the sake of simplicity, fore and hind legs were

considered of the same lengths ($m=b$).

Fig. 7 shows that if the robot length (parameter a) increases, then the robot step ΔL decreases. Additionally, the condition $a+m=\text{constant}$ means that the robot step increases when the length of the robot legs increases. The ideal robot must therefore have long legs and a short back.

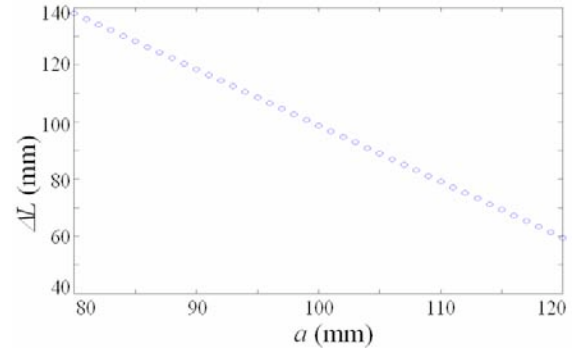


Fig. 7 The variation of L , ΔL , decreases when the variable (a) increases. The variables (a) and (m) are constrained by equation $a+m=\text{constant}$. The SMA wires can be contracted up to 4% of their length.

The second analysis focused on CGR back deflection during the contraction of the SMA wires. Since the CGR back is fixed differently to the fore and hind robotic legs (Fig. 2), the compliant back was modeled as a cantilever with an external normal force, R , and a moment, M , applied to its end (Fig. 8). Both R and M are functions of the cantilever deflection and their values were therefore computed in an iterative procedure during CGR back deflection. The effect of the distance spacer, s , on the distance, d , and force, F , (Fig. 8) was studied using large deflection theory [11].

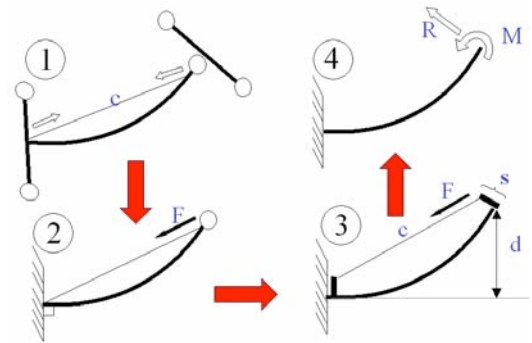


Fig. 8 Model for the SMA force analysis. The CGR can be reduced to the study of a cantilever contracted by a SMA wire. The distance spacer (s) introduces a variable moment M .

The flowchart in Fig. 9 shows the used iterative procedure. Parameters r_0 and F_0 , the approximated cantilever curvature and the estimated SMA constant force, respectively, represent the initial software inputs. For the sake of simplicity, Fig. 9 does not show all software subsystems, e.g. subsystems for computing elliptic integrals, which are involved in the cantilever large deflection computation.

Fig. 10 shows results obtained using realistic data of the CGR prototype back: Young's elastic modulus=226GPa; back length=10cm; back width=2.4cm. Fig. 10 is very

important in considering control strategies. In fact, the developed cantilever deflection model can be used in a feed-forward control loop.

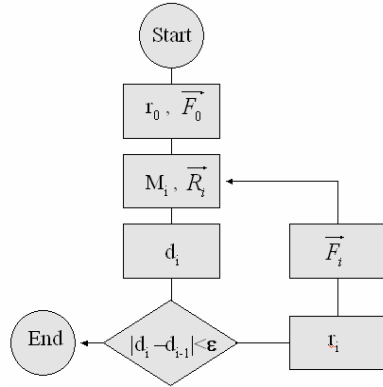


Fig. 9 Flowchart of the software developed for the iterative computation of CGR back deflection. Large deflection theory was used.

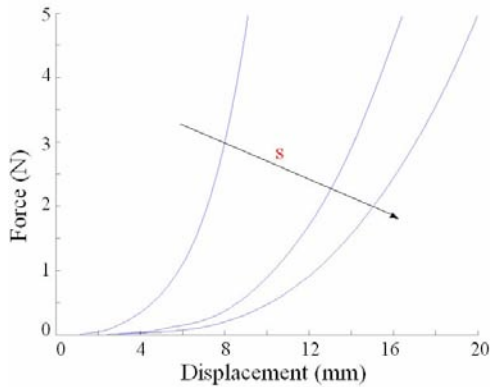


Fig. 10 Forces that the SMA wires exert for bending the CGR back. Different curves correspond to different values of the distance spacer s .

For the CGR locomotion design, weight and dynamic forces were neglected as the robot prototype was designed to be very light and to climb slowly.

III EXPERIMENTAL SYSTEMS

In this section, actual RGR and CGR prototypes are presented. Robot specifications and characteristics are also discussed.

III.A Rigid Gecko Robot Prototype

The chassis of the RGR, which was designed to operate in macroscale and for future space applications, was built using aluminum alloy. The robotic frame was obtained through folding techniques starting from aluminum sheets. RGR was equipped with five electrical solenoid motors, four for lifting the robotic legs, and one for the robot locomotion. The maximum torque of each motor, which was amplified by 81:1 gearboxes, was 25Nmm obtained using 5V. The RGR received off-board power and was controlled by a PIC 16F877 micro-controller integrated in a built-customized electronic board. Fig. 11 shows the control strategy used for one-full robot step. All five motors were controlled in a particular sequence in order to detach one foot per time minimizing the risk of robot falling.

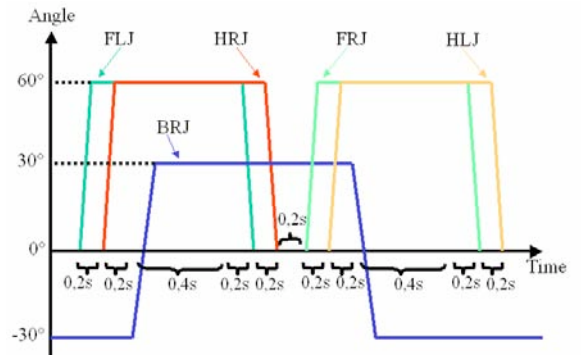


Fig. 11 Control Strategy for one-full robot step: time evolution of the rotations of each motorized joint.

III.B Compliant Gecko Robot Prototype

The fabrication of the CGR, shown in Fig. 12, was very challenging due to the use of SMA wires and composite material chassis. The CGR back was equipped with 50 m diameter SMA wires with a transition temperature of about 90°C (Flexinol® high temperature SMA wires). Several thin wires were used instead of few thick wires in order to increase the natural convection effect during SMA wires' cooling phase. For the heating phase, an external power system was used. The maximum contraction of the wires was 0.6cm, 6% of their length (10cm), and was obtained using 5V. The thermal cycle rate was 1cyc/s.

The CGR chassis was built with a composite structure made of the following three layers:

1. Unidirectional prepreg glass fiber (S2Glass) having 30 m thickness.
2. Prepreg carbon fiber (M60J) weaves having 80 m thickness.
3. Unidirectional glass fiber (S2Glass) having 3cm thickness.

The use of glass fiber had two different purposes: 1) Reinforcing the compliant body structure; 2) Electrically isolating the CGR frame when in contact with SMA wires. A thin layer of epoxy, obtained by the use of a spinner machine, was also spread over the composite robot back in order to increase the electrical isolation.

Composite material theory was used to compute the mechanical properties of the CGR back laminate (Table 1).

Table 1

E_1 (GPa)	E_2 (GPa)	G_{12} (GPa)	ν_{12}
226	205	7	0.3

The final CGR back was 2.4cm wide and 12cm long. Six SMA wires, which were fixed on each side of the robot, were able to bend the CGR back and provide robot locomotion. Three composite material failure theories (Tsai-Hill, Hoffman, and Tsai-Wu [12]) were used to structurally verify the CGR compliant back when bent by SMA wires.

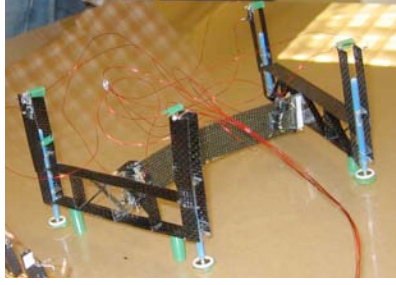


Fig. 12 Photo of the Compliant Gecko Robot prototype

The construction of the middle revolute joint (Fig. 5 and Fig. 6) was carried out using a compliant joint of PDMS. Robot legs were controlled using 100 μ m diameter SMA wires which had 0.7cyc/s thermal cycle rate. The leg configurations made it possible to use long SMA wires (14cm) able to lift the robot feet up to 0.5cm. The CGR received off-board power.

The RGR and CGR have comparable sizes but the technological solutions which were developed for the CGR allow a feasible robotic miniaturization by simply scaling down the already built prototype.

IV TEST RESULTS

The RGR had a robust behavior while walking in a horizontal plane showing a gait similar to Gecko. Fig. 13 shows three RGR snap-shots during the climbing phase.

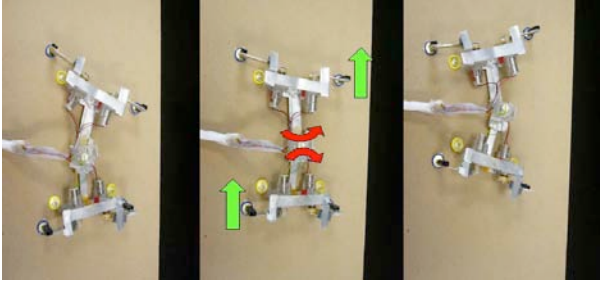


Fig. 13 Snap-shots of the RGR while it climbs a surface inclined at 65°.

RGR characteristics are shown in Table 2.

Table 2 RGR performance results and characteristics

Rigid Gecko Robot	
Weight (g)	80
Length (cm)	10
Width (cm)	10
Speed (cm/s)	2
Power Consumption (mW)	360
Slope Angle (degrees)	65

The maximum speed, 2cm/s, was mainly limited by software parameters. A speed of 6cm/s is expected by modifying the control law. The RGR was able to climb, in any direction, an acrylic surface inclined at 65° with respect to a horizontal plane. The performance of the robot, which was potentially able to climb a vertical surface, was mainly limited by the absence of encoders for the feedback control of the leg positions. The use of encoders can also reduce the RGR power consumption. In fact, motors could be turned off when the legs are lifted

and turned on only for attaching and detaching phases. This strategy would allow the robot to consume 130mW.

Static and dynamic tests were also carried out on the Compliant Gecko Robot, in order to characterize the compliant back behavior. The measurement equipment included a laser scan micrometer able to measure displacements of the compliant back during SMA wires' contraction. The resolution of the micrometer was of 2 μ m. The length of the compliant back was of 12cm.

Fig. 14 shows the SMA wire voltage as a function of CGR back displacements d (see also Fig. 8). Even though Fig. 14 and Fig. 10 have different y-axes, they can be compared since the voltage applied to SMA wires is proportional to the force that the wires exert. In a steady air environment, the SMA wire force is proportional to the SMA wire temperature [13]. In addition, the relationship between temperature and voltage can be expressed as follows:

$$T = a_1 \cdot \left(\frac{V}{\rho \cdot D} \right) + a_2 \cdot \left(\frac{V}{\rho \cdot D} \right)^2 \quad (2)$$

where ρ is the resistance of the SMA wire, D is the SMA wire diameter, V is the voltage applied to the SMA wire, and a_1 and a_2 are empirical constants. Since a_1 , whose value is about 0.7, is two orders of magnitude higher than a_2 (0.006), the second term of the above equation can be neglected. Since SMA voltage is proportional to SMA temperature, which is also proportional to SMA force, by the transitive property, SMA voltage and SMA force are proportional.

Experimental results of Fig. 14 are consistent with theoretical results of Fig. 10 suggesting the use of the model developed in section II.C, in a feed-forward control loop in order to predict compliant back behavior.

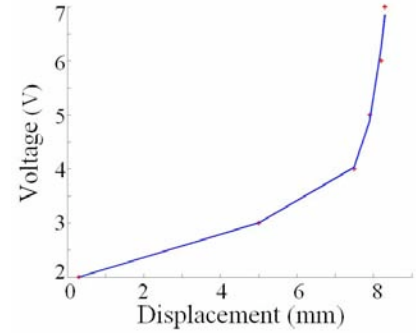


Fig. 14 Behavior of the CGR back during SMA wires' contraction

The dynamic behavior of the compliant back was characterized recording its displacement during SMA wire contractions. Fig. 15 shows the temporal evolution of the compliant back for both heating and cooling SMA phases using three different voltages. Analyzing Fig. 15:

1. If the SMA wire length is changed without intermissions, the cycling time is about 1 cyc/s.
2. Increasing the voltage from 4V to 6V, the maximum CGR back displacement increases only of 0.5mm.
3. The cooling phase had a dominant effect on the whole cycle time.

4. Increasing the voltage results in a jitter effect.

These considerations suggest the use of the minimum voltage necessary for obtaining a desired displacement. This is also the best condition for CGR power consumption.

An instability effect is observed when 5V are used: the graph in the middle of Fig. 15 shows that the first pick of the curve is lower than the second one. This instability is caused by the dynamic behavior of the SMA wires and the elastic compliant back. The contraction of the SMA wires bends and accelerates the CGR compliant back. The inertia force of the back temporarily overcomes the back elastic force. The compliant back starts to vibrate. The first oscillation is interrupted by the SMA wire action (point A in Fig. 15) which results in another contraction of the GCR compliant back. This instability can be reduced increasing the dumping and decreasing the mass of the compliant back. One possible solution is to replace the carbon fibers with aramidic fibers and lighten the laminate by reducing the epoxy in the composite matrix.

The performance and characteristics of the CGR are shown in Table 3. This robot, which was able to climb a 65° slanted surface, was manually controlled and thus the velocity (~0.3cm/s) and power consumption (~1W) were functions of the operator ability.

Table 3 CGR performance and characteristics

Compliant Gecko Robot	
Weight (g)	10
Length (cm)	10
Width (cm)	10
Slope Angle (degrees)	65

V CONCLUSIONS

The significance of realizing agile robots able to avoid obstacles and climb any kind of surfaces has driven the research to focus on the ability of animals able to climb vertical walls. The two developed prototypes which are presented in this paper, demonstrate the feasibility and capability of novel robot designs inspired by Gecko locomotion. Experimental results show that the two robots are potentially able to climb vertical surfaces although adhesive characteristics and uncontrolled leg positions limit their performance. The maximum slope of the climbed acrylic surface was 65°. The highest recorded speed was 2 cm/s, but 6 cm/s is the velocity expected by improving the control law of the guiding software. Future work includes miniaturization and implementation of new synthetic adhesives for space environment operations.

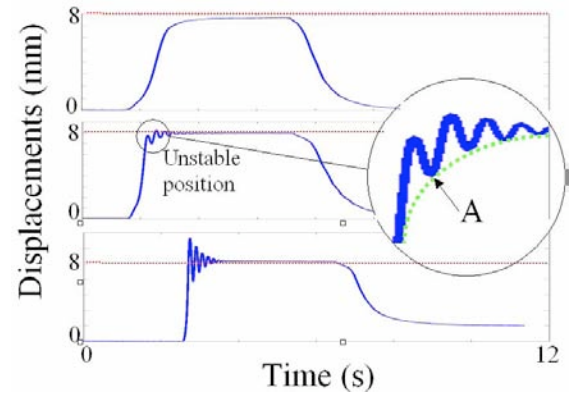


Fig. 15 Dynamic behavior of SMA wires using 5V

ACKNOWLEDGMENT

The authors thank to Burak Aksak for electronic board design, Eugene Cheung for experimental adhesive measurements, Ozgur Unver for rigid gecko robot fabrication, Murat Asci for robot foot fabrication, Sandy Hsieh for compliant robot tests, and especially Thomas Quentin Berna for compliant gecko robot fabrication.

REFERENCES

- [1] L. Briones, P. Bustamante, and M. Serna, "ROBICEN: A wall-climbing pneumatic robot for inspection in nuclear power plants," *Robotics and Computer-Integrated Manufacturing*, vol. 11, pp. 287-9, 1994.
- [2] K. Yesin, B. Nelson, N. Papanikolopoulos, R. Voyles, and D. Krantz, "Active Video System for a Miniature Reconnaissance Robot," *Proc. of the IEEE Int. Conf. on Robotics and Automation*, pp. 3920-25, 2000.
- [3] S. Hirose, A. Nagakubo, and R. Toyama, "Machine that can walk and climb on floors, walls and ceilings," *Proc. of the Int. Conf. on Advanced Robotics*, pp. 753-8, 1991.
- [4] S. Martel, P. Madden, L. Sosnowski, I. Hunter, and S. Lafontaine, "NanoWalker: a fully autonomous highly integrated miniature robot for nano-scale measurements", *Proc. of the SPIE Int. Symp. on EnviroSense, Microsystems Metrology and Inspection*, p. 3825, Germany, 1999.
- [5] Y. Jiao, S. Gorb, and M. Scherge, "Adhesion measured on the attachment pads of *tettigonia viridissima* (orthoptera, insecta)," *Journal of Experimental Biology*, vol. 203, pp. 1887-1895, 2000.
- [6] K. Autumn, Y. Liang, T. Hsieh, W. Zesch, W.P. Chan, T. Kenny, R. Fearing, and R.J. Full, "Adhesive force of a single gecko foot hair," *Nature*, 405, pp. 681-5, 08 June 2000.
- [7] R.T. Pack, J.L. Christopher, K. Kawamura, "A Rubbertuator-Based Structure-Climbing Inspection Robot," *Proceedings of the IEEE Conference on Robotics and Automation*, pp. 1869-1874, 1997.
- [8] H.R. Choi, S.M. Ryew, T.H. Kang, J.H. Lee, and H.M. Kim, "A wall climbing robot with closed link mechanism", *Proc. of the Intelligent Robotic Systems Conference*, pp. 2006-2011, vol. 3, 2000.
- [9] C. Menon, M. Murphy, and M. Sitti, "Gecko Inspired Surface Climbing Robots" *Proc. of the IEEE International Conference on Robotics and Biomimetics (ROBIO)*, Shenyang, China, Aug 2004.
- [10] C.R. Hibbeler, "Structural analysis," Prentice Hall, 2001.
- [11] Larry L. Howell, "Compliant Mechanisms", *Wiley-Interscience*, 2001.
- [12] I.M. Daniel and O. Ishai, "Engineering Mechanics of Composite Materials," New York, Oxford, Oxford University Press, 1994.